Phytopathology Research

RESEARCH Open Access

Transcriptome analysis reveals pathways facilitating the growth of tobacco powdery mildew in Arabidopsis

Ran Li[1], Ling-Li Zhang[1], Xue-Mei Yang[1], Xiao-Long Cao[1], Ying-Ge Wang[1], Xian-Feng Ma[1,2,4], Viswanathan Chandran[1], Jing Fan[1], Hui Yang[1,3], Jing Shang[1,3], Ji-Qun Zhao[1], Shunyuan Xiao[2], Yan Li[1] and Wen-Ming Wang[1*]

Abstract

Powdery mildew (PM) fungi are biotrophic pathogens that rely on living hosts to survive and thrive. However, their colonization is restricted by host defenses at both the penetration and post-penetration stages. The tobacco PM strain *Golovinomyces cichoracearum* (*Gc*) SICAU1 has overcome penetration resistance of Arabidopsis but its growth is arrested by post-penetration resistance. While *Gc* SICAU1 only poorly grows in Arabidopsis Col-0 wild-type plants, it can sustainably grow for more than 20 days on the same infected leaves of the double mutant *pad4–1 sid2–1* that is defective in both the synthesis and signaling of salicylic acid (SA). To understand the underlying molecular mechanisms, we conducted a comparative transcriptome analysis between Col-0 and *pad4–1 sid2–1* in response to *Gc* SICAU1. We found that 4811 genes were differentially expressed more than four-fold between any two of the measured seven time points (0, 1, 3, 6, 8, 10 and 12 days post-inoculation). Gene expression pattern analysis suggests that differential expression of 348 genes and 190 genes may explain resistance in Col-0 and susceptibility in *pad4–1 sid2–1*, respectively. Gene Ontology (GO) analysis suggests that *Gc* SICAU1 might be arrested in Col-0 by both pattern-triggered immunity and SA-dependent defense. By contrast, its sustained growth in *pad4–1 sid2–1* may be attributable to the activation of a detoxification pathway that is normally repressed by the SA-signaling pathway. Taken together, our results suggest that multiple distinct, yet interconnected pathways control the growth of tobacco powdery mildew in Arabidopsis.

Keywords: Basal defense, SA-signaling, Post-penetration defense, Pattern-triggered immunity, *Golovinomyces cichoracearum* SICAU1, Detoxification

Background

Powdery mildew (PM) diseases epidemically occur in nearly 10,000 plant species including many economically and agriculturally important crops (Kuhn et al. 2016). Successful colonization of a powdery mildew begins with germination of a conidium upon landing on the surface of a host plant, which is followed by the formation of an appressorium that further develops a penetration peg to break the host cell wall. At the tip of the penetration peg, it forms a feeding structure called the haustorium to steal photosynthates for its epiphytic growth (Kuhn et al. 2016). During the infection processes, the host plant mounts spatiotemporally distinct defenses to stop the invasion of the pathogen. The first line of defense is penetration resistance, which is essentially mounted by the rigid host cell wall as a physical barrier; attempted fungal penetration induces the formation of the papilla, i.e. cell wall apposition, enriched for callose at the penetration site (Collins et al. 2003; Assaad et al. 2004). Using Arabidopsis-powdery mildew interaction as a model phytopathosystem, it has been demonstrated that papilla formation may be part of pattern-triggered immunity (PTI), which is activated upon recognition of chitin by the pattern-recognition receptor CERK1 (CHITIN ELICITOR RECEPTOR-LIKE KINASE 1) together with LYK5 (LYSIN-MOTIF RECEPTOR LIKE KINASE 5)

* Correspondence: j316wenmingwang@sicau.edu.cn
[1]Rice Research Institute and Research Center for Crop Disease and Insect Pests, Sichuan Agricultural University at Wenjiang, Chengdu 611130, China
Full list of author information is available at the end of the article

(Miya et al. 2007; Cao et al. 2014). Consistently, the *cerk1* mutant is more susceptible to the adapted PM *Golovinomyces cichoracearum* than the wild type (Wan et al. 2008). Application of chitin results in callose deposition at the treated tissue (Underwood and Somerville 2013). Conversely, loss-of-function mutations in *PENETRATION 1* (*PEN1*) lead to delayed formation of the papilla and increased penetration rate of the non-host powdery mildew pathogen *Blumeria graminis* f. sp. *hordei* in Arabidopsis (Collins et al. 2003; Assaad et al. 2004). Accumulation of callose as a major constituent of papillae requires the callose synthase PMR4/GSL5 (POWDERY MILDEW RESISTANCE 4 / GLUCAN SYNTHASE LIKE 5) (Nishimura et al. 2003). Although loss-of-function in *PMR4* leads to enhanced resistance to adapted PM, which may be due to compensatory activation of SA-dependent defense, overexpression of *PMR4* or the GTPase *RabA4c* enhances callose deposition to the papilla, leading to complete penetration resistance to PM (Ellinger et al. 2013; Eggert et al. 2014; Ellinger et al. 2014). Indeed, the formation of a callose encasement of the haustorium complex (EHC) was observed in some invaded epidermal cells of Col-0, an Arabidopsis accession susceptible to an adapted PM (Wang et al. 2009), but the frequency of EHC formation is much higher in plants challenged with a non-adapted PM (Wen et al. 2011), implying that adapted PM pathogen can suppress callose deposition and more effectively break penetration resistance to establish colonization. Not surprisingly, the frequency of EHC is significantly increased in plants expressing *RESISTANCE TO POWDERY MILDEW8* genes (including *RPW8.1* and *RPW8.2*). Moreover, the expression of *RPW8.2* can be induced to mediate cell death and the RPW8.2 protein is specifically targeted to the extra-haustorial membrane (EHM) encasing the haustorium (Wang et al. 2009), which nicely explains why RPW8 mediates broad-spectrum resistance to PM. Apparently, RPW8.2 activates EHM-based, post-penetration resistance including enhanced EHC formation against adapted PM (Kuhn et al. 2016).

Certain host genes are required for successful pathogenesis of PM and thus act as susceptibility factors. Loss-of-function in such genes can result in enhanced disease resistance to PM. For example, some plant mutants display resistance to adapted PM pathogens that were impaired for potential PM susceptibility. Such mutants include *edr* (*enhanced disease resistance*), *pmr* (*powdery mildew resistance*) and *mlo* (*mildew locus O*) mutants of Arabidopsis, barley or wheat (Buschges et al. 1997; Frye et al. 2001; Vogel et al. 2002; Nishimura et al. 2003; Tang et al. 2005; Consonni et al. 2006; Tang et al. 2006; Wang et al. 2014; Wu et al. 2015). Therefore, it is feasible to engineer disease resistance in crops by identifying and editing susceptibility factors.

The tobacco powdery mildew strain *Gc* SICAU1 is a poorly-adapted pathogen to Arabidopsis. Although it can finish its life cycle in the Arabidopsis wild type Col-0, its growth is arrested because of post-penetration defense (Zhang et al. 2015). Nevertheless, the double mutant *pad4–1 sid2–1* can support its growth to more than 20 days which is unusually long because vigorous PM growth in a compatible host normally lasts for 12–15 days before the collapse of the infected leaves, indicating that the mutant not only lacks the post-penetration defense, but some pathways are activated to support the sustained growth of the PM strain (Zhang et al. 2015). Thus, *PAD4* (*PHYTOALEXIN DEFICIENT 4*) and *SID2* (*SALICYLIC ACID INDUCTION DEFICIENT 2*) are important for post-penetration resistance to tobacco powdery mildew in Arabidopsis. PAD4 interacts directly with EDS1 (ENHANCED DISEASE SUSCEPTIBILITY 1) to mediate basal defense and SA-signaling-dependent disease resistance (Zhou et al. 1998; Rusterucci et al. 2001). *SID2* encodes the isochorismate synthase acting in SA biosynthesis (Nawrath and Metraux 1999). Thus, Arabidopsis-*Gc* SICAU1 interactions could be an ideal pathosystem to dissect the mechanism of sustained growth of PM in Arabidopsis.

In the present study, to understand why loss of *PAD4* and *SID2* results in unusually long sustained growth of tobacco powdery mildew in *pad4–1 sid2–1*, we performed a comparative transcriptome analysis between Col-0 and *pad4–1 sid2–1* upon *Gc* SICAU1 inoculation. Our data confirmed that basal defense and SA-signaling-associated pathways contribute to post-penetration defense against tobacco powdery mildew. Moreover, a detoxification pathway contributes to the sustained growth of tobacco PM in Arabidopsis.

Results

The number of genes responsive to tobacco powdery mildew is quite different between Col-0 and *pad4–1 sid2–1*

Previously, we isolated a tobacco powdery mildew strain, *Gc* SICAU1, which poorly sporulated in Arabidopsis ecotype Col-0 (Zhang et al. 2015). However, it can grow in the double mutant *pad4–1 sid2–1* abundantly as in its host tobacco plants (Fig. 1). To understand the underlying mechanism, we performed a time course transcriptome analysis by collecting samples at 0, 1, 3, 6, 8, 10, and 12 days post inoculation (dpi) with two biological replicates for RNA-seq. Data from the two biological replicates were highly consistent as demonstrated by the correlation coefficient matrix between samples (Additional file 1: Figure S1a). Clean reads were mapped to TAIR10 reference genome. Both unique mapped rate and total mapped rate exhibited the following features: in the samples collected from before and at 3 dpi, the unique mapped rates for both Col-0 and *pad4–1 sid2–1* were quite similar, being of about ~ 78% and the total

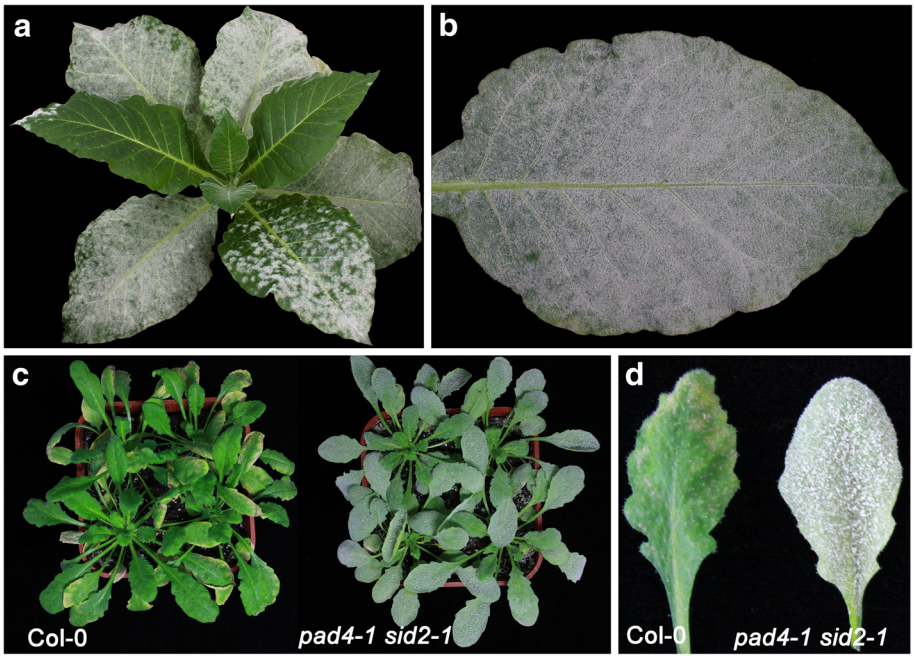

Fig. 1 Powdery mildew disease phenotypes in tobacco and Arabidopsis. Powdery mildew disease phenotypes in a representative tobacco plant **(a)**, leaf (**b**), indicated Arabidopsis plants **(c)** and leaves **(d)** at 12 dpi of the tobacco powdery mildew isolate *Golovinomyces cichoracearum* SICAU1

mapped rates of about ~ 93% (Additional file 2: Table S1 and Additional file 1: Figure S1b, c). However, at and after 6 dpi in the mutant, the unique mapped rates and total mapped rates reduced over the time course and were lower than that in Col-0 (Additional file 2: Table S1 and Additional file 1: Figure S1b, c). The reduced percentage of mapped reads in *pad4–1 sid2–1* could be due to the increase of the pathogen at the later time points.

To identify the genes showing the most differential response to *Gc* SICAU1, we selected the differentially expressed genes (DEGs) at variations of absolute Log_2 fold change ≥2 and a false discovery rate ≤ 0.01 between any two time points. Subsequently, there were 4811 DEGs identified (Additional file 3: Table S2). Then, the DEGs were further screened by comparison between different time points and 0 dpi in Col-0 and in *pad4–1 sid2–1*, respectively. Compared to 0 dpi, the number of up-regulated genes increased from 255 genes at 1 dpi to 1101 genes at 12 dpi in Col-0, and from 176 genes at 1 dpi to 741 genes at 12 dpi in *pad4–1 sid2–1* (Fig. 2a, b). Conversely, the number of down-regulated genes reduced from 494 genes at 1 dpi to 344 genes at 8 dpi, and then increased to 650 genes at 12 dpi in Col-0; whereas, the number of down-regulated genes reduced from 592 genes at 1 dpi to 433 genes at 8 dpi, and then increased to 630 genes at 12 dpi in *pad4–1 sid2–1* (Fig. 2a, b). Obviously, there were more up-regulated genes in Col-0 than in *pad4–1 sid2–1* at 1, 3, 10 and 12 dpi, but more up-regulated genes in *pad4–1 sid2–1* than in Col-0 at 6 and 8 dpi; whereas, there were more down-regulated genes in *pad4–1 sid2–1* than in Col-0 at 1–10 dpi, but similar number at 12 dpi (Fig. 2a, b).

Because the DEGs obtained during the time course could be due to either the aging of the plants or the infection of the pathogen, we also compared the number of DEGs between Col-0 and *pad4–1 sid2–1* at each time point. At 0 dpi, there were 26 genes expressed higher and 62 genes expressed lower in *pad4–1 sid2–1* than in Col-0 (Fig. 2c). Over the time course of infection, the number of higher- and lower-expressed genes was increased, particularly, a sudden increase occurred to the number of higher-expressed genes in *pad4–1 sid2–1* at 6 dpi and to the number of lower-expressed genes at 3 dpi (Fig. 2c). The higher-expressed genes in *pad4–1 sid2–1* could contribute to the sustained growth of *Gc* SICAU1, whereas, the lower-expressed genes in *pad4–1 sid2–1* could reflect the lack of post-penetration defense in *pad4–1 sid2–1* and thus contribute to post-penetration defense in Col-0. Therefore, these data indicate that 3 dpi may be critical for transcriptome-reprogramming to defend against the pathogen and 6 dpi may be critical to establish the sustained growth of the pathogen.

The number of genes contributes to post-penetration defense in Col-0 and susceptibility in *pad4–1 sid2–1*

To identify the genes most likely associated with post-penetration resistance in Col-0 and susceptibility in *pad4–1 sid2–1*, we further performed comparison between

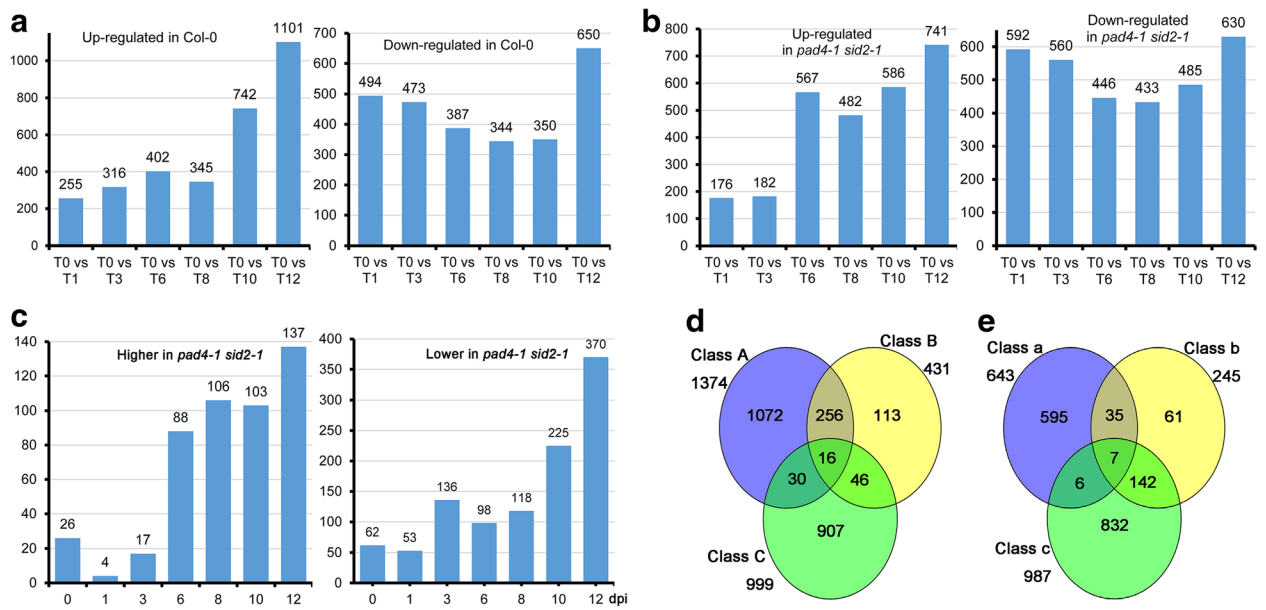

Fig. 2 Number of differentially expressed genes over the time course of infection and between Col-0 and *pad4–1 sid2–1*. **a** Number of up-regulated and down-regulated genes in Col-0 at the indicated time points from 1 dpi (T1) to 12 dpi (T12) in comparison with un-inoculated plants (T0). **b** Number of up-regulated and down-regulated genes in *pad4–1sid2–1* at the indicated time points (from T1 to T12) in comparison with un-inoculated plants (T0). **c** Number of up-regulated and down-regulated genes in *pad4–1sid2–1* at the indicated dpi in comparison with Col-0 at the same time points. **d** Venn graph shows the gene numbers up-regulated in Col-0 (compared to 0 dpi, designated class A, blue cycle), down-regulated in *pad4–1sid2–1* (compared to Col-0, designated class B, yellow cycle) and down-regulated in *pad4–1sid2–1* (compared to 0 dpi, designated class C, green cycle). **e** Venn graph shows the gene numbers down-regulated in Col-0 (compared to 0 dpi, designated class a, blue cycle), up-regulated in *pad4–1sid2–1* (compared to Col-0, designated class b, yellow cycle) and up-regulated in *pad4–1 sid2–1* (compared to 0 dpi, designated class c, green cycle)

the DEGs by making two Venn diagrams. One Venn diagram was made by comparing the genes exhibiting up-regulation in Col-0 over the time course versus 0 dpi (Class A) with the genes showing down-regulation in *pad4–1 sid2–1* versus Col-0 at each time point (Class B), and the genes exhibiting down-regulation in *pad4–1 sid2–1* over the time course versus 0 dpi (Class C) (Fig. 2d). Another diagram was made by comparing the genes down-regulated in Col-0 over the time course versus 0 dpi (Class a) with the genes up-regulated in *pad4–1sid2–1* at each time point versus Col-0 (Class b), and the genes up-regulated in *pad4–1 sid2–1* over the time course versus 0 dpi (Class c) (Fig. 2e). The genes consensually up-regulated in Col-0 and down-regulated in *pad4–1 sid2–1* could be those contributing to post-penetration defense, whereas, the genes consensually upregulated in *pad4–1 sid2–1* could contribute to susceptibility in the mutant. The data showed that there were 16 genes consensually detected in the Classes A, B and C, whereas,256 genes in the Classes A and B, 30 genes in the Classes A and C, and 46 genes in the Classes B and C (Fig. 2d and Additional file 4: Table S3). These genes could be the ones contributing to the defense in Col-0. On the other hand, there were 142 genes consensually detected in the Classes b and c, whereas, 35 genes in the Classes a and b, 7 genes in the Classes a, b and c, and 6 genes in the Classes a and c (Fig. 2e and Additional file 5: Table S4). These genes could be the ones contributing to the sustained growth of the pathogen in *pad4–1 sid2–1*.

Taken together, there are 348 genes that might contribute to the activation of post-penetration defense against the tobacco PM strain *Gc* SICAU1 in Col-0. Whereas, 190 genes may contribute to the susceptibility in *pad4–1 sid2–1*.

Categories of biological processes from GO analysis on DEGs contribute to post-penetration defense in Col-0 and susceptibility in *pad4–1 sid2–1*

In order to identify the biological functions contributing the most to post-penetration defense in Col-0 and susceptibility in *pad4–1 sid2–1*, we performed Gene Ontology (GO) analyses on the DEGs over the time course of infection of *Gc* SICAU1. Our results showed that the genes expressed higher in Col-0 than in *pad4–1 sid2–1* were mainly enriched in 25 biological processes (Table 1). Whereas, the genes expressed higher in *pad4–1 sid2–1* than in Col-0 were enriched in 20 biological processes (Table 1).

The 25 biological processes that may contribute to post-penetration defense in Col-0 can be further classified into three classes. Class I contained three categories of GO biological process terms, including receptor

Table 1 GO enrichment of genes expressed higher in Col-0 or in *pad4–1 sid2–1* over the time course

GO term	Total	Higher in Col-0							Higher in *pad4–1 sid2–1*						
		T0	T1	T3	T6	T8	T10	T12	T0	T1	T3	T6	T8	T10	T12
PTI															
Receptor protein kinase signaling pathway	522			15	9	10	20	33							
MAPK cascade	86	8	10	13	10	10	14	20							
Protein kinase activity	1110	17		31	19	22	34	56							
SA-associated															
SA-mediated signaling pathway	62			7	4	4	7	12							
SA biosynthetic process	79	13	8	18	11	13	16	26							
Systemic acquired resistance	125	12	9	27	18	23	26	34							
Response to SA	152	5	6	9	7	9	15	18							
JA-mediated signaling pathway	99	5	5	9	8	9	13	18							
Defense response	464	7		10				19							
Defense response to fungus	488	11	13	24	16	17	26	34					8		
Defense response, incompatible interaction	41		4	4	4	4	4	8							
Regulation of defense response	66		4	8	5	6	7	8							
Regulation of plant-type HR	121	5	5	12	7	7	11	17							
Senescence	64		2		2	2		6							
Others															
Response to chitin	234	6	5	11	6		14	27	5			7	8	5	3
Protein targeting to membrane	124	5	5	12	7	7	11	17							
Response to ER stress	82		4	7	6	6	7	9							
Response to oxidative stress	260						12	14							
Calcium ion binding	282			8		7	10	14							
ATP binding	2406			28				56							
Abscisic acid-activated signaling pathway	215							11							
Plasmodesma	1369			29	16	17	29	50							
Apoplast	449			10	8	10	12						8		
Detection of biotic stimulus	25	7	4	9	6	7	9	13							
Vacuole	572			12											
Detoxification															
Toxin catabolic process	89											8	6	4	4
Response to toxic substance	67											8	3	4	5
Proline transport	38											6	4	5	4
Amino acid transport	53											4	3	4	2
Glutathione transferase activity	53											5	2	3	3
Flavonoid biosynthetic process	144											6	4	6	7
Flavonoid glucuronidation	114											6	3	4	4
Flavonol biosynthetic process	12												2	2	3
UDP-glucosyltransferase activity	24											5	3	2	
Intracellular membrane-bounded organelle	157											7	3	4	5
Quercetin 3-O-glucosyltransferase activity	112											6	3	4	4
Secondary metabolism															
Apoplast	449											8	8	6	6
Chitin binding	25											3	3	2	3

Table 1 GO enrichment of genes expressed higher in Col-0 or in *pad4–1 sid2–1* over the time course *(Continued)*

GO term	Total	Higher in Col-0							Higher in *pad4–1 sid2–1*						
		T0	T1	T3	T6	T8	T10	T12	T0	T1	T3	T6	T8	T10	T12
Chitin catabolic process	26											3	4	2	3
Chitinase activity	25											3	3	2	3
Indole glucosinolate metabolic process	25												4	1	2
Response to nitrate	81											2	5	3	3
Response to other organism	27											3	3	6	7
Cellular response to hydrogen peroxide	4											2	2	1	
Intracellular membrane-bounded organelle	157											7	3	4	5

protein kinase signaling pathway, MAPK cascade and protein kinase activity, which mainly belong to PTI (Table 1 and Additional file 6: Table S5). In this class, we detected high induction of some receptor genes such as *LYK5* (*AT2G33580*), *WAK1* (*AT1G21250*), *RLK5* (*AT4G28490)*, *RLP23* (*AT2G32680*), together with 16 cysteine-rich receptor-like protein kinases (CRKs), 11 receptor-like proteins (RLPs), three receptor kinases (RKs), two receptor-like kinases (RLKs) and one L-type Lectin Receptor Kinase (LECRK) (Additional file 6: Table S5). Further screening of DEGs identified 26 CRKs whose expression changed more than 4-fold between any 2 time points (Additional file 7: Table S8). Class II included 11 GO biological process terms (Table 1). In this class, four terms related to "SA signaling pathway", including salicylic acid biosynthetic process, systemic acquired resistance, SA-mediated signaling pathway and response to SA, and there were 46 genes in this category with higher expression in Col-0 than in *pad4–1 sid2–1* (Additional file 6: Table S6). Six genes from SA signaling pathway was also enriched in the JA-signaling pathway (Additional file 6: Table S6). In addition, there were eight more genes enriched in JA-signaling pathway (Additional file 6: Table S6). We used the category "defense response" to include all genes enriched in the biologic processes of the GO terms defense response, defense response to fungus and defense response in incompatible interaction. There were 30 genes in this category, of which 14 genes expressed higher in Col-0 than in *pad4–1 sid2–1* at all tested time points and nine genes were at the highest expression at 12 dpi (Additional file 6: Table S6). Class III contained the rest of the 11 biological processes (Table1). Taken together, genes involved in PTI- and SA-associated pathways were expressed higher in Col-0 than in *pad4–1 sid2–1*.

The 20 biological processes that may contribute to the sustained growth of the tobacco powdery mildew in *pad4–1 sid2–1* were further classified into "detoxification" and "secondary metabolism" (Table 1 and Additional file 6: Table S7). The "detoxification" class contained genes associated with the detoxification pathway, including 13 genes in the term of toxin catabolic process/response to toxic substance, of which four encode GSTUs (Glutathione S-Transferase), two encode UGTs (UDP-Glucose Transferase) and one encodes CYP (Cytochrome P450 monooxygenase); seven genes in the term proline transport/amino acid transport/glutathione transferase activity and nine genes involved in flavonoid biosynthetic process/flavonoid glucuronidation/flavonol biosynthetic process (Additional file 6: Table S7). Totally, seven *UGT* genes were differentially induced over the time course of infection of *Gc* SICAU1 with expression higher in *pad4–1 sid2–1* than in Col-0 (Additional file 6: Table S7). Intriguingly, while *UGT76E11* (*AT3G46670*) was expressed higher in *pad4–1 sid2–1* than in Col-0 over the time course of infection, the other six *UGT* genes, i.e. *UGT73B3* (*AT4G34131*), *UGT73B4* (*AT2G15490*), *UGT73B5* (*AT2G15480*), *UGT73C1* (*AT2G36750*), *UGT74E2* (*AT1G05680*) and *UGT75B1* (*AT1G05560*), were expressed higher in Col-0 than in *pad4–1 sid2–1* at one to three time points before 3 dpi, but higher in *pad4–1 sid2–1* than in Col-0 at 6–12 dpi (Additional file 6: Table S7). In addition, we also detected the other 27 UGTs that were differentially expressed in Col-0 and *pad4–1 sid2–1* upon infection of *Gc* SICAU1, most of them expressed higher in *pad4–1 sid2–1* than in Col-0 (Additional file 8: Table S9). There were seven genes encoding apoplast proteins, eleven genes responsive to chitin/chitin binding or involved in chitin catabolic process, and two genes functioning in indole glucosinolate metabolic process (Additional file 6: Table S7). These genes provide the opportunity to further dissection of the mechanism in plant-powdery mildew interactions.

Expression patterns over the time course of infection classify genes contributing to post-penetration defense in Col-0 and susceptibility in *pad4–1 sid2–1*

To be more accurate in demonstrating the expression patterns of the genes involved in post-penetration defense in Col-0 and susceptibility in *pad4–1 sid2–1*, we performed analysis on the expression pattern of genes for the consensually up-regulated or down-regulated genes in Col-0 and *pad4–1 sid2–1*. First, we performed

clustering analysis on all the DEGs that were classified into 119 clusters (Additional file 9: Figure S2). Then we further analyzed the clusters containing the consensually up-regulated or down-regulated genes in Col-0 and *pad4–1 sid2–1*. Subsequently, the clusters contributing to resistance were classified into four groups, i.e. Resistance group A (R_A), R_B, R_C and R_D, each represented by 8 clusters (Fig. 3). R_A included clusters 13, 48, 53, 57, 73, 75, 84 and 110 with an obviously up-regulated expression in Col-0 but not much change in *pad4–1 sid2–1* over the time course (Fig. 3a). R_B included clusters 17, 30, 70, 72, 74, 82, 85 and 104 with a pattern of up-regulation over the time course but higher in Col-0 than in *pad4–1 sid2–1* (Fig. 3b). R_C included clusters 7, 8, 10, 28, 4, 83, 96 and 98 with patterns of slightly up-regulation over the time course in both Col-0 and *pad4–1 sid2–1* with expression higher in Col-0 than in *pad4–1 sid2–1* (Fig. 3c). R_D included clusters 16, 39, 60, 61, 69, 86, 113 and 117 with patterns that the expression were decreased over the time course of infection, but the expression were higher in Col-0 than in *pad4–1 sid2–1* (Fig. 3d).

Meanwhile, we also classified the DEGs up-regulated in *pad4–1 sid2–1* into five susceptibility groups. Susceptibility group A (S_A) was represented by clusters 5, 47, 92, 97, 102, 106 and 107, whose expression was obviously up-regulated in *pad4–1 sid2–1*, particularly at and after 6 dpi of *Gc* SICAU1 but not much change in Col-0 (Fig. 4a). S_B was represented by clusters 9, 22, 31, 34, 88, 91, 108 and 114 with expression increased over the time course of infection but higher in *pad4–1 sid2–1* than in Col-0 (Fig. 4b). S_C was represented by clusters 21, 35, 37 and 101 with patterns of expression increased over the time course but higher in *pad4–1 sid2–1* than in Col-0 at and after 6 dpi of *Gc* SICAU1 (Fig. 4c). S_D was represented by clusters 52, 58, 93 and 111 with patterns of expression decreased upon inoculation of *Gc* SICAU1, but the expression was higher in *pad4–1 sid2–1* than in Col-0 (Fig. 4d). S_E was represented by clusters 1, 6, 42 and 44 with patterns of expression increased at 1–6 dpi and then dropped back at later time points but the expression was higher in *pad4–1 sid2–1* than in Col-0 (Fig. 4e).

Reverse-transcription quantitative PCR confirmed the RNA-seq data

To validate the RNA-seq data, we conducted an independent time course experiment and collected samples for reverse-transcription quantitative PCR (RT-qPCR) on 19 genes selected from some resistance and susceptibility groups. Four genes from R_A, including *PR1* (*AT2G14610*), *BGL2* (*AT3G57260*), *PR5* (*AT1G75040*) and *DLO1* (*AT4G10500*), were highly up-regulated in Col-0 upon infection of *Gc* SICAU1 but only slightly up-regulated at later time points in *pad4–1 sid2–1* (Fig. 5a). Four genes from R_B, including *EFR72* (*AT3G16770*), *PR4* (*AT3G04720*), *NATA1* (*AT2G39030*) and *ST2A* (*AT5G07010*), were up-regulated in both Col-0 and *pad4–1 sid2–1* upon infection of *Gc* SICAU1 with expression higher in Col-0 than in *pad4–1 sid2–1* at most of the tested time points (Fig. 5b). Five genes from R_C were examined by RT-qPCR, of which four genes, including *HCHIB* (*AT3G12500*), *ORA59* (*AT1G06160*), *SEN4* (*AT4G30270*) and *NAC6* (*AT5G39610*), were up-regulated in both Col-0 and *pad4–1 sid2–1* upon infection of *Gc* SICAU1 with expression higher in Col-0 than in *pad4–1 sid2–1* in most of the tested time points (Fig. 5c). Nevertheless, *PDF1.2* (*AT5G44420*) from R_C was up-regulated higher in Col-0 than in *pad4–1 sid2–1* at 1 and 3 dpi, but higher in *pad4–1 sid2–1* than in Col-0 at and after 6 dpi (Fig. 5d). *AT3G05730*, a gene encoding a defensin-like family protein, was not classified into the R or S group, exhibiting an pattern of low expression at earlier time points but up-regulated in Col-0 and *pad4–1 sid2–1* at and after 6 dpi with expression higher in Col-0 than in *pad4–1 sid2–1* at 6, 8 and 10 dpi, higher in *pad4–1 sid2–1* at 12 dpi (Fig. 5d). Two genes from S_C were examined of which *WRKY6* (*AT1G62300*) was up-regulated in both Col-0 and *pad4–1 sid2–1* with expression higher in *pad4–1 sid2–1* than in Col-0 at 3 and 8 dpi, whereas, the expression of *SEN1* (*AT4G35770*) was higher in *pad4–1 sid2–1* at all examined time points except 10 dpi (Fig. 5e). Three genes from S_A were examined with expression higher in *pad4–1 sid2–1* than in Col-0 (Fig. 5f). Apart from some genes at certain time points (11 of 133) that were not consistent with the RNA-seq data, which could be due to the systemic error occurred between different experiments, most of the time points (122 of 133) in the examined genes were consistent with the RNA-seq data (Additional file 3: Table S2). Therefore, our RNA-seq data were reliable and should be significant for future investigation.

Discussion

Multiple pattern-triggered immune pathways may constitute the basal defense preventing the growth of tobacco powdery mildew in Col-0

In this study, over a time course of infection by a poorly-adapted tobacco powdery mildew strain in Arabidopsis, we detected high induction of genes in receptor protein kinase signaling pathway, MAPK cascade and protein kinase activity, such as *LYK5*, *WAK1*, *RLK5*, *RLP23* and 16 *CRK* genes, indicating that multiple PTI pathways may be involved in preventing the growth of tobacco powdery mildew in Col-0. First, chitin is a major component of fungal cell wall, presenting in conidia and at the tips of growing hyphae of powdery mildew (Ramonell et al. 2005). The chitin receptor gene *LYK5* encodes a LysM-containing receptor-like kinase. Upon cognition of chitin, LYK5 forms a complex with CERK1

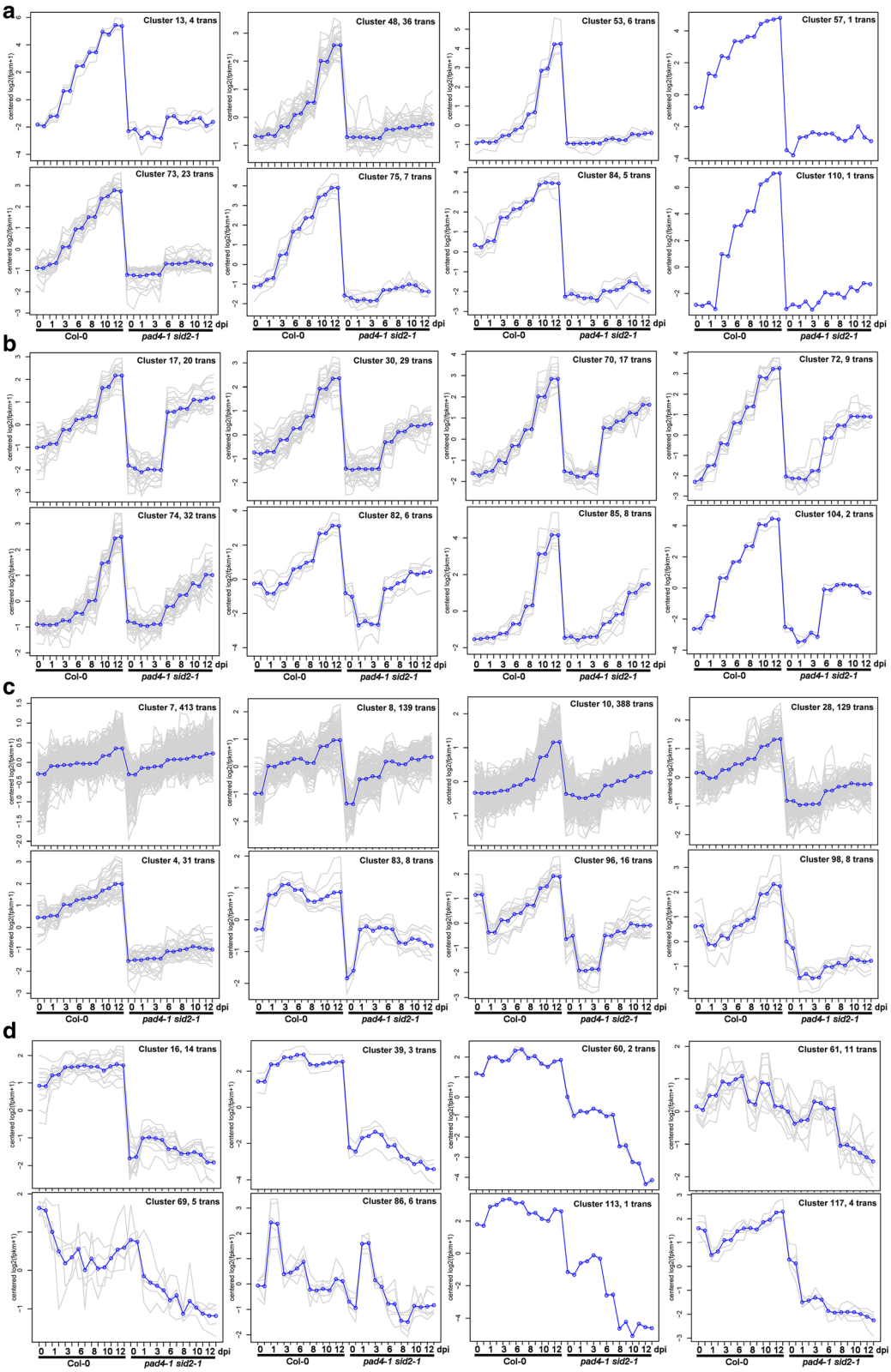

Fig. 3 (See legend on next page.)

(See figure on previous page.)
Fig. 3 Four types of clustered DEGs involved in post-penetration defense. **a** Resistance type A clusters with DEGs up-regulated in Col-0 but no obvious change in *pad4–1 sid2–1*. **b** Resistance type B clusters with DEGs up-regulated in Col-0 but delayed up-regulation in *pad4–1 sid2–1*. **c** Resistance type C clusters with DEGs up-regulated in both Col-0 and *pad4–1sid2–1* but the up-regulation in *pad4–1sid2–1* are lower than that in Col-0. **d** Resistance type D clusters with DEGs expressed highly in Col-0 and down-regulated in *pad4–1sid2–1*

to activate down-stream innate immunity (Cao et al. 2014). Therefore, chitin-triggered immunity could be one contribution to the post-penetration defense against tobacco powdery mildew in Col-0 (Fig. 6). Second, Wall-associated Kinase 1 (WAK1) acts as a receptor of oligogalacturonides (OGs) derived from the plant cell wall after wound (Brutus et al. 2010; Gramegna et al. 2016). Here, we detected that *WAK1* was expressed higher in Col-0 than in *pad4–1 sid2–1* over the time course (Additional file 6: Table S5). This is consistent with its roles in response to wound because powdery mildew infection could cause wound on the host. Third, SOBIR1 forms a complex with the PRR protein RLP23 (AT2G32680), and recruits BAK1 into a tripartite complex upon recognizing necrosis- and ethylene-inducing peptide 1-like proteins (NLPs) that are produced by fungal, oomycete and bacterial pathogens to mediate immune activation (Albert et al. 2015). *SOBIR1* acts in both penetration and post-penetration resistance to the non-host fungal pathogen *Magnaporthe oryzae* in Arabidopsis (Takahashi et al. 2016). Thus, RLP23-SOBIR1-BAK1-mediated PTI signaling pathway may play roles in post-penetration defense against tobacco powdery mildew (Fig. 6). Fourth, RLK5/HAE (AT4G28490) is a receptor for the INFLORESCENCE DEFICIENT IN ABSCISSION (IDA)-derived peptide (Wang et al. 2017). Although its roles in response to fungal pathogen are not reported, we detected that *RLK5*/*HAE* was expressed higher in Col-0 than in *pad4–1 sid2–1* over the time course of infection (Additional file 6: Table S5), implying that RLK5-mediated PTI pathway may be involved in defense against tobacco powdery mildew (Fig. 6).

In addition, IOS1 (for IMPAIRED OOMYCETE SUSCEPTIBILITY 1, AT1G51800) plays critical roles in chitin-induced PTI via association with the PRR CERK1 and the co-PRR BAK1 (Yeh et al. 2016). SARD1 (At1g73805) and CBP60g (AT5G26920) are key regulators controlling SA synthesis via regulation of the expression of *ICS1*. In turn, the expression of *SARD1* and *CBP60g* is regulated by PCRK1 (AT3G09830) and PCRK2 who also interact with FLS2 (Kong et al. 2016). *SARD1* expression is also regulated by *WRKY70* (Zhou et al. 2018). Here, we found that *IOS1*, *SARD1* and *WRKY70* were expressed higher in Col-0 than in *pad4–1 sid2–1* (Additional file 6: Table S5 and Table S6). Therefore, IOS1-CERK1 may crosstalk with SARD1-CBP60g through PRRs and contribute to basal defense against tobacco powdery mildew (Fig. 6).

Finally, CRKs are one large subfamily of RLKs with 44 members in Arabidopsis and play important roles in response to abiotic and biotic stresses (Wrzaczek et al. 2010). We detected 16 *CRK*s that were expressed higher in Col-0 than in *pad4–1 sid2–1* over the time course of infection, including *CRK1*, *CRK4*, *CRK5*, *CRK6*, *CRK7*, *CRK8*, *CRK14*, *CRK15*, *CRK23*, *CRK24*, *CRK26*, *CRK36*, *CRK37*, *CRK38*, *CRK39* and *CRK45* (Additional file 6: Table S5 and Additional file 7: Table S8). Previously, *CRK4*, *CRK5*, *CRK6*, *CRK7*, *CRK8*, *CRK14*, *CRK15*, *CRK23*, *CRK24*, *CRK36*, *CRK37*, *CRK38* and *CRK39* were found to be associated with cell death in *bak1*/*serk4* mutant through regulation of ER quality control (ERQC) (de Oliveira et al. 2016). Overexpression of certain *CRK*s, such as *CRK4*, *CRK5*, *CRK13*, *CRK19* and *CRK20*, can induce cell death in Arabidopsis transgenic plants (Chen et al. 2003; Chen et al. 2004; Acharya et al. 2007; de Oliveira et al. 2016). Moreover, overexpression of other *CRK*s, such as *CRK4*, *CRK6* and *CRK36* also leads to enhanced PTI responses (Yeh et al. 2015). Some *CRK*s are associated with SA-signaling pathway. SA can induce the expression of *CRK4*, *CRK5*, *CRK6*, *CRK10*, *CRK11*, *CRK19*, *CRK20* and *CRK45*, while overexpression of *CRK5*, *CRK13* and *CRK20* results in higher amount of SA and up-regulation of *PR1*, *PR5* and *ICS1*, marker genes of the SA-signaling pathway (Chen et al. 2003; Acharya et al. 2007; Ederli et al. 2011; Zhang et al. 2013). Therefore, CRKs may also play roles in basal defense and cooperate with SA-signaling pathway to activate post-penetration defense against tobacco powdery mildew, and some of them may contribute to cell death at late infection stage in Col-0 (Fig. 6).

Taken together, our data indicate that multiple PTI signaling pathways may constitute post-penetration defense against tobacco powdery mildew in Arabidopsis (Fig. 6).

Many SA-signaling-associated genes are up-regulated in Col-0 upon *Gc* SICAU1 infection

Previously, several labs have reported that SA-signaling pathway is required for host defense against powdery mildew (Nishimura et al. 2003; Xiao et al. 2005; Fabro et al. 2008). SA-signaling pathway also contributes to post-penetration defense against tobacco powdery mildew in Arabidopsis (Zhang et al. 2015). Here, we detected many SA-signaling-associated genes that were expressed higher in Col-0 than in *pad4–1 sid2–1*. First, several well-known SA-signaling pathway marker genes were expressed much higher in Col-0 than in *pad4–1 sid2–1* upon infection of *Gc* SICAU1, including the *Pathogenesis-Related gene 1* (*PR1*), *PR2* (*BGL2*), *PR5*,

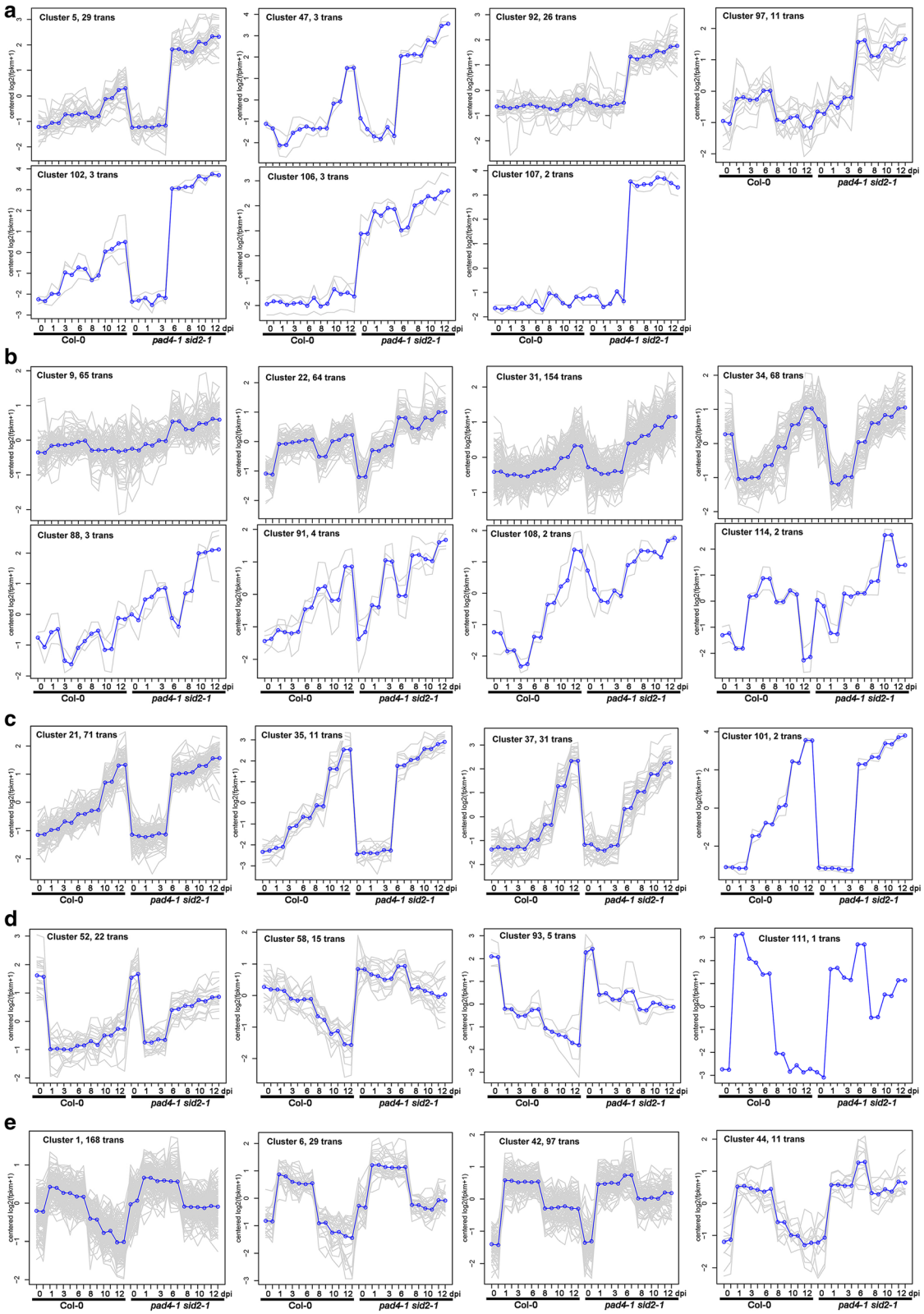

Fig. 4 (See legend on next page.)

(See figure on previous page.)
Fig. 4 Five types of clustered DEGs involved in susceptibility to powdery mildew. **a** Susceptibility type A clusters of DEGs dramatically up-regulated in *pad4–1 sid2–1* particularly at and after 6 dpi but no obvious change or only slightly up-regulated in Col-0. **b** Susceptibility type B clusters of DEGs up-regulated in both Col-0 and *pad4–1 sid2–1* but the up-regulation in *pad4–1sid2–1* are higher than that in Col-0. **c** Susceptibility type C clusters of DEGs up-regulated in both Col-0 and *pad4–1 sid2–1* but dramatically up-regulated in *pad4–1sid2–1* particularly at and after 6 dpi. **d** Susceptibility type D clusters of DEGs expressed higher in *pad4–1sid2–1* than in Col-0 but down-regulated upon powdery mildew infection. **e** Susceptibility type E clusters of DEGs up-regulated in both Col-0 and *pad4–1 sid2–1* at 1~6 dpi and then dropped back at 8~12 dpi with expression higher in *pad4–1sid2–1* than in Col-0

DLO1, *DOX1*, *NIMIN1*, *PHYTOALEXIN DEFICIENT 3* (*PAD3*), *ACD6* and *LURP1*, and the SA synthetic pathway genes *SID2* and *EDS5* (Fig. 5a and Additional file 6: Table S6). Second, SA-signaling pathway associates with many WRKY transcription factors. We detected 7 WRKY transcription factors, i.e. *WRKY38* (*AT5G22570*), *WRKY51* (*AT5G64810*), *WRKY53* (*AT4G23810*), *WRKY54* (*AT2G40750*), *WRKY58* (*AT3G01080*), *WRKY62* (*AT5G01900*) and *WRKY70* (*AT3G56400*), whose expression were higher in Col-0 than in *pad4–1 sid2–1* over the time course (Additional file 6: Table S6). While *WRKY70* acts as an activator of SA-signaling pathway but a repressor of JA-signaling pathway, *WRKY38* and *WRKY62* negatively regulate SA-signaling pathway, *WRKY53* and *WRKY54* are SA-responsive transcription factor acting as a positive and negative regulator of leaf senescence, respectively (Li et al. 2004; Li et al. 2006; Kim et al. 2008; Besseau et al. 2012). The expression of *WRKY70* is positively regulated by the R2R3 Myb family TF *MYB44* (*AT5G67300*) (Shim et al. 2013). Consistently, we found that *MYB44* was down-regulated in both Col-0 and *pad4–1 sid2–1* over the time course (Additional file 4: Table S3). Third, the Glutaredoxin-encoding gene *GRX480* associates with TGA transcription factors and is involved in SA/JA cross-talk by suppressing JA-responsive *PDF1.2* transcription (Ndamukong et al. 2007). *GRXS13* is also required to maintain proper levels of superoxide radicals to protect cells from oxidative damage (Laporte et al. 2012). Here, we detected that the expression of *GRX480* and *GRX13* were higher in Col-0 than in *pad4–1 sid2–1* over the time course (Additional file 6: Table S6). Fourth, *Downy Mildew Resistant 6* (*DMR6*) and its closest homologs *DMR6-Like Oxygenase*s (*DLO*s), *DLO1* and *DLO2*, are responsive to SA. They negatively promote susceptibility to the downy mildew *Hyaloperonospora arabidopsidis*, the bacterium *P. syringae* and the oomycete *Phytophthora capsici* (Zeilmaker et al. 2015). Here, both *DMR6* and *DLO1* were up-regulated in Col-0, but down-regulated in *pad4–1 sid2–1* upon infection of *Gc* SICAU1 (Additional file 6: Table S6 and Additional file 4: Table S3), implying that they play roles in response to tobacco powdery mildew.

Detoxification pathway may play critical roles for the sustained growth of tobacco powdery mildew in *pad4–1 sid2–1*

To scavenge the endogenous and/or exogenous toxic substances, most organisms exploit a three-phase detoxification system (Lallement et al. 2014). In phase one, enzymes such as cytochrome P450 monooxygenases (CYPs) catalyze reactions to introduce a functional moiety to hydrophobic substrates. In phase two, the newly modified substrates are conjugated with glutathione by specific classes of GSTs. Then the glutathionylated products are either sequestered in the vacuole or exported to the apoplast. Therefore, CYPs, hyroxylases and peroxidases act as the major players in phase 1, GSTs and glycosyl transferease act in phase 2, whereas, exocytosis and apoplastic signaling are required in phase 3. In our transcriptome data, we detected 3 CYP, 5 GST, 7 UGT genes, and 7 genes in apoplastic signaling that were expressed higher in *pad4–1 sid2–1* than in Col-0 (Additional file 6: Table S7). While CYPs, GSTs, and UGTs may act in phase 1–2, apoplastic signaling genes may act in phase 3. Thus, our data imply that the sustained growth of *Gc* SICAU1 in *pad4–1 sid2–1* may rely on the activation of the detoxification pathway (Fig. 6).

Secondary metabolites are involved in diverse stress-induced responses. These compounds rarely accumulate in their free form but are often conjugated to Glc through the action of glycosyltransferases that are encoded by *UGT* gene family. *UGT* members are involved in stress-induced responses (Langlois-Meurinne et al. 2005). Here, we detected seven *UGT* genes that were induced over the time course of infection with expression higher in *pad4–1 sid2–1* than in Col-0 (Additional file 6: Table S7) and the other 27 UGTs that were differentially expressed in Col-0 and *pad4–1 sid2–1* upon infection of *Gc* SICAU1, most of them expressed higher in *pad4–1 sid2–1* than in Col-0 (Additional file 8: Table S9). Among them, *UGT78D1* (*AT1G30530*) encodes a UDP-rhamnose:flavonol-3-Orhamnosyltransferase involved in flavonol glycoside biosynthesis (Jones et al. 2003). Interestingly, most of the above mentioned *UGT*s belong to Arabidopsis Glycolsytransferase Family 1 that were reported to be significantly up-regulated by treatment of 2,4,6-trinitrotoluene (TNT) (Gandia-Herrero et al. 2008). Therefore, UGT-mediated detoxification pathway genes may play roles for the

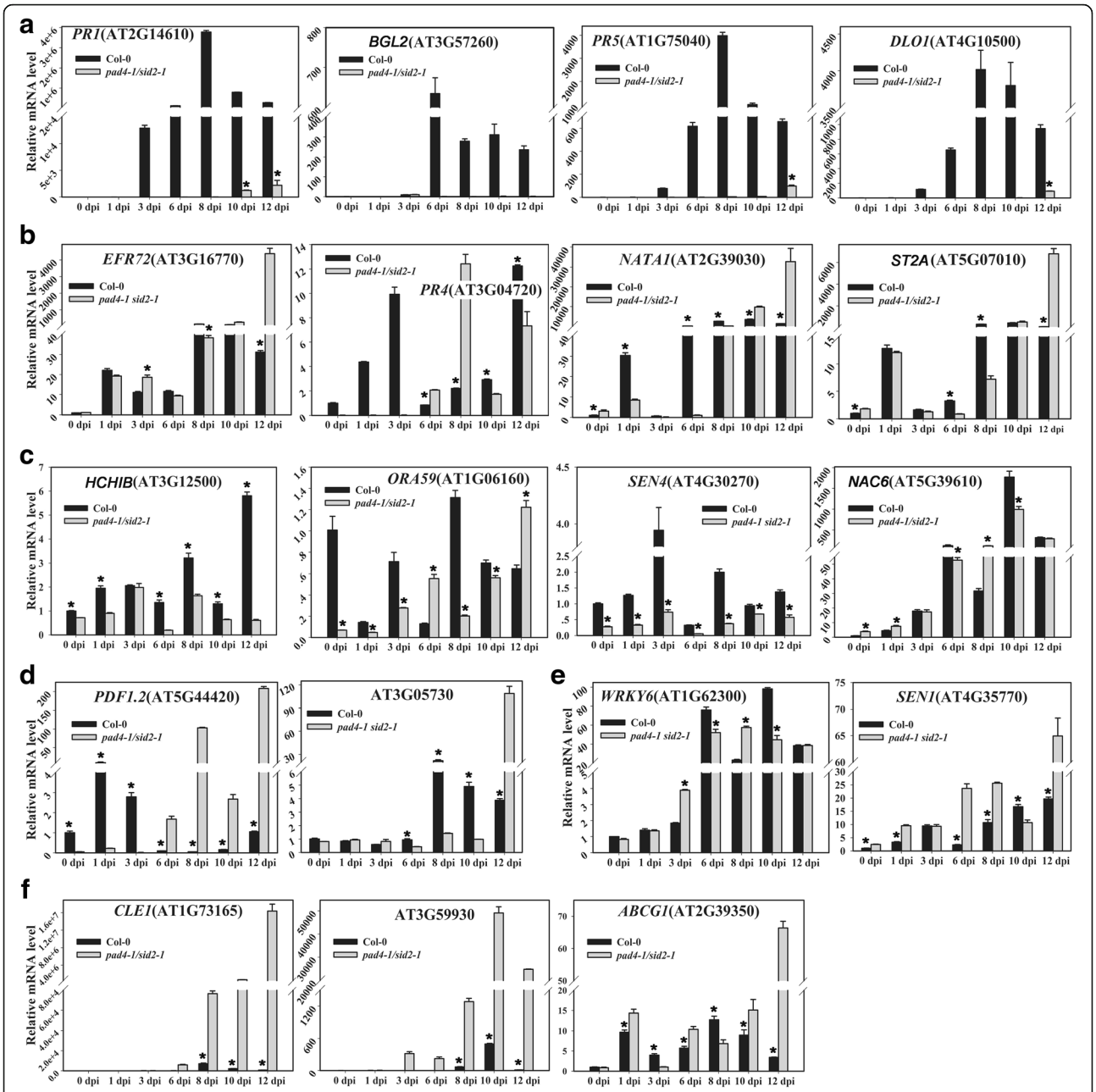

Fig. 5 Validation of some DEGs by RT-qPCR. Reverse transcription quantitative PCR (RT-qPCR) analysis on the relative mRNA levels of the indicated four representative resistance type A genes (**a**), four representative resistance type B genes (**b**), four representative resistance type C genes (**c**), one representative resistance type C gene and one gene not in the classified group (**d**), two representative susceptibility type C genes (**e**), three representative susceptibility type A genes (**f**). Note in (**a**) that the mRNA levels were highly induced at and after 3 dpi in Col-0, but remained at low levels in *pad4–1 sid2–1*, and in (**f**) that the mRNA levels of *CLE1* and *At3g59930* were remarkably up-regulated at and after 6 dpi in *pad4–1 sid2–1*. Relative mRNA levels were normalized to 0 dpi of Col-0 that was arbitrarily set as 1. Values are means of three technique replications. Error bars indicate SD. Asterisks above the bars indicate significant differences between Col-0 and *pad4–1 sid2–1* at $P < 0.01$ as determined by student's *t*-test. All the experiments were repeated two times with similar results

sustained growth of *Gc* SICAU in the *pad4–1 sid2–1* mutant (Fig. 6).

CLE (*CLAVATA3*/*Endosperm surrounding region-related*) family genes encode secreted peptides acting in regulation of plant growth, development and response to environmental stimuli (Wang et al. 2015). Previously, *CLE1* was found to act in signaling regulating root development in nitrogen-dependent manner (Araya et al. 2014). In our data, we identified that *CLE1* (*AT1G73165*) was highly and particularly induced in *pad4–1 sid2–1* from 6 to 12 dpi (Fig. 5f and

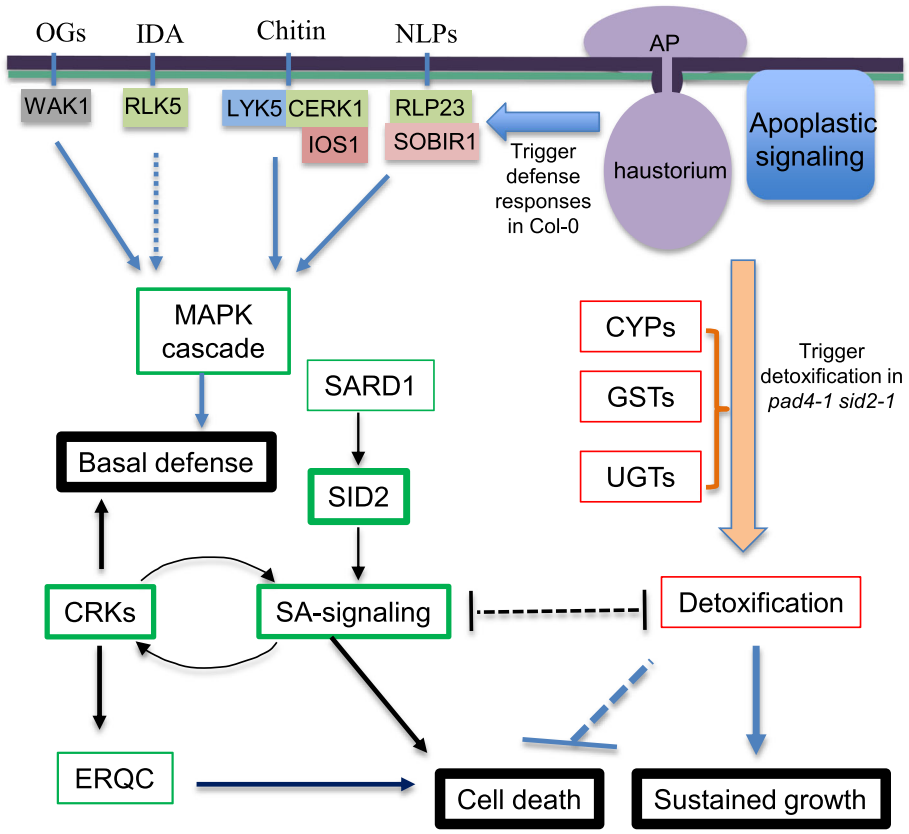

Fig. 6 Hypothetic working model for activation of post-penetration defense or sustained growth of tobacco powdery mildew in Arabidopsis

Additional file 6: Table S7). Thus, *CLE1* may play a role in apoplast signaling to regulate the sustained growth of *Gc* SICAU in *pad4–1 sid2–1* mutant and this could be an interesting focus in future research.

It seems that the genes involved in the detoxification pathway were also activated in Col-0 at earlier time points (1–3 dpi) but dropped back to background level presumably due to the activation of defense-related signaling pathways. Particularly, SA signaling pathway might suppress the activation of detoxification. On the contrary, genes involved in detoxification may be continually increased in *pad4–1 sid2–1* due to the lack of SA signaling (Fig. 6).

Conclusions

Powdery mildew fungi are complex pathogens that infect many agriculturally important plants such as wheat, barley and rye. In a previous study, we identified the tobacco PM strain *Gc* SICAU1 that can grow well in *pad4–1 sid2–1* but not in Col-0 (Zhang et al. 2015). Here, through transcriptome analysis on a time course of infection, we found that 3 dpi was important for activation of post-penetration defense in Col-0 and 6 dpi was crucial for activation of the detoxification pathway for the sustained growth in *pad4–1 sid2–1*. We also identified a number of genes that may contribute to post-penetration defense and the sustained growth. From these data and combining with the function of related genes reported in the literatures, we proposed a working hypothesis for the post-penetration defense in Col-0 and the sustained growth in *pad4–1 sid2–1* (Fig. 6). First, upon infection of the tobacco powdery mildew in Col-0, a series of defense pathways may be activated. Quite a few receptors, such as LYK5, WAK1, RLP13 and RLK5, that recognize chitin, OGs, NLPs and IDA, respectively, were induced over the time course of infection. Subsequently, genes involved in MAPK cascade were also up-regulated, which in turn presumably led to activating basal defense. Meanwhile, a batch of CRKs was up-regulated, which probably led to activation of SA-signaling pathway. Eventually, these defense responses were culminated into cell death, which arrested the growth of the tobacco powdery mildew. On the contrary, because basal defense and SA-signaling were defective in *pad4–1 sid2–1*, a variety of genes involved in the detoxification pathway were remarkably up-regulated particularly at and after 6 dpi of *Gc* SICAU1. The detoxification pathway may be antagonistic to SA-signaling pathway and presumably recruited members of CYP, GST and UGT gene families that are involved in toxin catabolic process,

proline/amino acid transport, flavonoid biosynthetic process and apoplastic signaling. In turn, the detoxification pathway led to the sustained growth of *Gc* SICAU1 in *pad4–1 sid2–1*. In theory, genes involved in the sustained growth of *Gc* SICAU1 could be the candidates for engineering disease resistance by gene-knock-out approaches and thus are significant in future investigations.

Methods

Plant materials and powdery mildew inoculation

Arabidopsis thaliana wild type (WT) accession Col-0 and the double mutant *pad4–1 sid2–1* were grown under 8 h/16 h light/dark regime at 22 °C. Tobacco powdery mildew isolate *Gc* SICAU1 was maintained on tobacco leaves at 23 °C (16 h light, 8 h dark) in a growth room as previously reported (Zhang et al. 2015). Rosette leaves from 6-week-old plants were inoculated with powdery mildew strain *Gc* SICAU1. Inoculum was prepared by growing of *Gc* SICAU1 on tobacco leaves for 10 days, and then spores were collected to inoculate on WT and *pad4–1 sid2–1*. Samples were collected at 0, 1, 3, 6, 8, 10 and 12 dpi for transcriptome analysis.

RNA-seq analysis

RNA was extracted from two biologically duplicated leaf samples using TRIzol® Reagent (Life Technologies, USA) following the manufacturer's protocol. RNA quantity and quality were determined using a 2100 BioAnalyzer (Agilent Technologies Canada Inc., Mississauga, ON, Canada). RNA libraries were constructed with 2 μg total RNA and subjected to high-throughput sequencing by a HiSeq-4000 sequencer (Illumina). Approximately 6 Gb of reads for each sample were obtained. After filtering the raw reads by removing adapter and reads with 5% "N", clean data were mapped to the TAIR10 reference genome by TopHat2 with default parameters (Kim et al. 2013).

The gene quantity was calculated by HTseq (Anders et al. 2015). The FPKM (Fragments Per Kilobase of transcript per Million fragments mapped) method (Lee et al. 2011) was used to calculate the normalized expression data of each gene (Mortazavi et al. 2008). DEGs were selected by DEseq2 (Love et al. 2014), with the criteria of absolute $\log_2$ fold change ≥2 and false discovery rate (FDR) ≤ 0.01 between any two samples. GO (Ashburner et al. 2000) database was used for gene ontology analysis. GO enrichment analysis was performed using GOseq (Young et al. 2010).

Clustering DEGs

Hierarchical clustering analysis of DEGs was run with hclust in R version 3.2.0. The FPKM of genes were log-converted and centered, and the complete linkage method was used. The median of $\log_2$(FPKM+ 1) for each transcript was subtracted from the $\log_2$(FPKM+ 1) value of each sample. Then the distance matrix was run with hclust in R, and a dendrogram was plotted that displays a hierarchical relationship among the vehicles. The hclust function in R uses the complete linkage method for hierarchical clustering by default. At every stage of the clustering process, the two nearest clusters were merged into a new cluster. The process was repeated until the whole data set was agglomerated into one single cluster. The final clusters were generated by cutting trees at 20% of the height.

Quantitative RT-PCR analysis

To validate the transcriptome data, reverse-transcription quantitative PCR (RT-qPCR) was performed for 19 genes representing different expression patterns. cDNA was synthesized from 0.5 μg total RNA using ReverTraAce qPCR RT Master Mix with gDNA Remover (TOYOBO, Japan). A two-step real-time PCR reaction was performed using an QuantiFast™ SYBR® QPCR kit (QIAGEN, Germany) with 100 ng template DNA and 10 nM each primer in a final volume of 10 μL according to the following protocol: polymerase activation at 95 °C for 5 min followed by denaturation at 95 °C for 10 s and concurrent annealing and extension at 65 °C for 30 s. The Arabidopsis actin (*ACT2*) gene was used as the internal control. Primer sequences were listed in Additional file 10: Table S10.

Additional files

Additional file 1: Figure S1. Analysis on the RNA-seq Data. **a** Sample correlation matrix. The correlation coefficient between two samples was indicated by color (color key) at the matrix. Note that the correlation coefficient between any two replicates was more than 0.95 (red squares at the diagonal line). Leaves with two biological replicates from Col-0 (Col) and *pad4–1 sid2–1* (ps) were collected at 0 (T0), 1 (T1), 3 (T3), 6 (T6), 8 (T8), 10 (T10) and 12 (T12) dpi of the tobacco powdery mildew strain *Golovinomyces cichoracearum* SICAU1 for RNA-seq-based transcriptome analysis. **b, c** Graphs show the reads number and total mapped reads for samples from Col-0 (**b**) and *pad4–1 sid2–1* (**c**). (JPG 3122 kb)

Additional file 2: Table S1. Summary of RNA-seq data (XLSX 12 kb)

Additional file 3: Table S2. List of differentially expressed genes with more than 4-fold change between any two samples (XLSX 1204 kb)

Additional file 4: Table S3. List of DEGs up-regulated in Col-0 (XLSX 164 kb)

Additional file 5: Table S4. List of DEGs up-regulated in *pad4–1 sid2–1* (XLSX 98 kb)

Additional file 6: Table S5. Genes involved in PTI expressed higher in Col-0 than in *pad4–1 sid2–1*. **Table S6.** SA-signaling-associated genes expressed higher in Col-0 than in *pad4–1 sid2–1*. **Table S7.** Genes expressed higher in *pad4–1 sid2–1* than in Col-0 at and after 6 dpi of Gc SICAU1 (DOCX 73 kb)

Additional file 7: Table S8. List of Cysteine-rich receptor-like protein kinases differentially expressed in Col-0 and *pad4–1 sid2–1* (XLSX 25 kb)

Additional file 8: Table S9. List of differentially expressed UGT genes in *pad4–1 sid2–1* and Col-0 (XLSX 23 kb)

Additional file 9: Figure S2. Clustering of deferential expressed genes responsive to tobacco powdery mildew. Hierarchical clustering analysis of DEGs generated 119 clusters. (JPG 8144 kb)

Additional file 10: Table S10. Primers for qRT-PCR in this study (XLSX 10 kb)

Abbreviations

AP: Appressorium; CRK: Cysteine-rich receptor-like protein kinase; CYP: Cytochrome P450 monooxygenase; DEG: Differentially expressed gene; EHC: Encasement of haustorium complex; EHM: Extra-haustorial membrane; ER: Endoplasmic reticulum; ERQC: Endoplasmic reticulum quality control; *Gc*: *Golovinomyces cichoracearum*; GO: Gene Ontology; GST: Glutathione S-transferase; IDA: Inflorescence deficient in abscission; JA: Jasmonic acid; MAPK: Mitogen-activated protein kinase; NLP: Necrosis and ethylene-inducing peptide 1-like protein; OG: Oligogalacturonides; PM: Powdery mildew; PTI: Pattern-triggered immunity; SA: Salicylic acid; SAR: Systemic acquired resistance; UGT: UDP-glucose transferase

Acknowledgements

We are grateful to Dr. Zhong-Xu Chen (Chengdu OnMath Technology Co., Ltd.) for RNA-seq analysis, Xinnan Wang for reading and correcting the manuscript.

Funding

This work was supported by the National Natural Science Foundation of China grants (31672090 and 31371931) to W-MW and the National Science Foundation grant (IOS-1146589 and IOS-1457033) to SX

Availability of data and materials

Not applicable.

Authors' contributions

RL, L-LZ, X-MY, X-LC, Y-GW, X-FM, HY, JS and J-QZ conducted the experiments. W-MW, SX, JF and YL supervised the study. W-MW, RL and VC wrote the manuscript. SX and W-MW polished the manuscript. W-MW coordinated the overall study. All authors read and approved the final manuscript.

Ethics approval and consent to participate

Not applicable.

Consent for publication

Not applicable.

Competing interests

The authors declare that they have no competing interests.

Author details

[1]Rice Research Institute and Research Center for Crop Disease and Insect Pests, Sichuan Agricultural University at Wenjiang, Chengdu 611130, China. [2]Institute for Bioscience and Biotechnology Research & Department of Plant Science and Landscape Architecture, University of Maryland, Rockville, MD 20850, USA. [3]College of Agronomy, Sichuan Agricultural University at Wenjiang, Chengdu 611130, China. [4]Hunan Provincial Key Laboratory for Germplasm Innovation and Utilization of Crop, Hunan Agricultural University, Changsha 410128, China.

Received: 19 September 2018 Accepted: 20 January 2019
Published online: 06 February 2019

References

Acharya BR, Raina S, Maqbool SB, Jagadeeswaran G, Mosher SL, Appel HM, et al. Overexpression of CRK13, an Arabidopsis cysteine-rich receptor-like kinase, results in enhanced resistance to *Pseudomonas syringae*. Plant J. 2007;50:488–99.

Albert I, Bohm H, Albert M, Feiler CE, Imkampe J, Wallmeroth N, et al. An RLP23-SOBIR1-BAK1 complex mediates NLP-triggered immunity. Nat Plants. 2015;1:15140.

Anders S, Pyl PT, Huber W. HTSeq—a python framework to work with high-throughput sequencing data. Bioinformatics. 2015;31:166–9.

Araya T, Miyamoto M, Wibowo J, Suzuki A, Kojima S, Tsuchiya YN, et al. CLE-CLAVATA1 peptide-receptor signaling module regulates the expansion of plant root systems in a nitrogen-dependent manner. Proc Natl Acad Sci U S A. 2014;111:2029–34.

Ashburner M, Ball CA, Blake JA, Botstein D, Butler H, Cherry JM, et al. Gene ontology: tool for the unification of biology. The Gene Ontology Consortium. Nat Genet. 2000;25:25–9.

Assaad FF, Qiu JL, Youngs H, Ehrhardt D, Zimmerli L, Kalde M, et al. The PEN1 syntaxin defines a novel cellular compartment upon fungal attack and is required for the timely assembly of papillae. Mol Biol Cell. 2004; 15:5118–29.

Besseau S, Li J, Palva ET. WRKY54 and WRKY70 co-operate as negative regulators of leaf senescence in *Arabidopsis thaliana*. J Exp Bot. 2012;63: 2667–79.

Brutus A, Sicilia F, Macone A, Cervone F, De Lorenzo G. A domain swap approach reveals a role of the plant wall-associated kinase 1 (WAK1) as a receptor of oligogalacturonides. Proc Natl Acad Sci U S A. 2010;107: 9452–7.

Buschges R, Hollricher K, Panstruga R, Simons G, Wolter M, Frijters A, et al. The barley *Mlo* gene: a novel control element of plant pathogen resistance. Cell. 1997;88:695–705.

Cao Y, Liang Y, Tanaka K, Nguyen CT, Jedrzejczak RP, Joachimiak A, et al. The kinase LYK5 is a major chitin receptor in Arabidopsis and forms a chitin-induced complex with related kinase CERK1. elife. 2014;3:e03766. https://doi.org/10.7554/eLife.

Chen K, Du L, Chen Z. Sensitization of defense responses and activation of programmed cell death by a pathogen-induced receptor-like protein kinase in Arabidopsis. Plant Mol Biol. 2003;53:61–74.

Chen K, Fan B, Du L, Chen Z. Activation of hypersensitive cell death by pathogen-induced receptor-like protein kinases from Arabidopsis. Plant Mol Biol. 2004;56:271–83.

Collins NC, Thordal-Christensen H, Lipka V, Bau S, Kombrink E, Qiu JL, et al. SNARE-protein-mediated disease resistance at the plant cell wall. Nature. 2003;425:973–7.

Consonni C, Humphry ME, Hartmann HA, Livaja M, Durner J, Westphal L, et al. Conserved requirement for a plant host cell protein in powdery mildew pathogenesis. Nat Genet. 2006;38:716–20.

de Oliveira MV, Xu G, Li B, de Souza VL, Meng X, Chen X, et al. Specific control of Arabidopsis BAK1/SERK4-regulated cell death by protein glycosylation. Nat Plants. 2016;2:15218.

Ederli L, Madeo L, Calderini O, Gehring C, Moretti C, Buonaurio R, et al. The *Arabidopsis thaliana* cysteine-rich receptor-like kinase CRK20 modulates host responses to *Pseudomonas syringae* pv. *tomato* DC3000 infection. J Plant Physiol. 2011;168:1784–94.

Eggert D, Naumann M, Reimer R, Voigt CA. Nanoscale glucan polymer network causes pathogen resistance. Sci Rep. 2014;4:4159.

Ellinger D, Glockner A, Koch J, Naumann M, Sturtz V, Schutt K, et al. Interaction of the Arabidopsis GTPase RabA4c with its effector PMR4 results in complete penetration resistance to powdery mildew. Plant Cell. 2014;26:3185–200.

Ellinger D, Naumann M, Falter C, Zwikowics C, Jamrow T, Manisseri C, et al. Elevated early callose deposition results in complete penetration resistance to powdery mildew in Arabidopsis. Plant Physiol. 2013;161: 1433–44.

Fabro G, Di Rienzo JA, Voigt CA, Savchenko T, Dehesh K, Somerville S, et al. Genome-wide expression profiling Arabidopsis at the stage of *Golovinomyces cichoracearum* haustorium formation. Plant Physiol. 2008; 146:1421–39.

Frye CA, Tang D, Innes RW. Negative regulation of defense responses in plants by a conserved MAPKK kinase. Proc Natl Acad Sci U S A. 2001;98: 373–8.

Gandia-Herrero F, Lorenz A, Larson T, Graham IA, Bowles DJ, Rylott EL, et al. Detoxification of the explosive 2,4,6-trinitrotoluene in Arabidopsis: discovery of bifunctional O- and C-glucosyltransferases. Plant J. 2008;56: 963–74.

Gramegna G, Modesti V, Savatin DV, Sicilia F, Cervone F, De Lorenzo G. GRP-3 and KAPP, encoding interactors of WAK1, negatively affect defense responses induced by oligogalacturonides and local response to wounding. J Exp Bot. 2016;67:1715–29.

Jones P, Messner B, Nakajima J, Schaffner AR, Saito K. UGT73C6 and UGT78D1, glycosyltransferases involved in flavonol glycoside biosynthesis in *Arabidopsis thaliana*. J Biol Chem. 2003;278:43910–8.

Kim D, Pertea G, Trapnell C, Pimentel H, Kelley R, Salzberg SL. TopHat2: accurate alignment of transcriptomes in the presence of insertions, deletions and gene fusions. Genome Biol. 2013;14:R36.

Kim KC, Lai Z, Fan B, Chen Z. Arabidopsis WRKY38 and WRKY62 transcription factors interact with histone deacetylase 19 in basal defense. Plant Cell. 2008; 20:2357–71.

Kong Q, Sun T, Qu N, Ma J, Li M, Cheng YT, et al. Two redundant receptor-like cytoplasmic kinases function downstream of pattern recognition receptors to regulate activation of SA biosynthesis. Plant Physiol. 2016; 171:1344–54.

Kuhn H, Kwaaitaal M, Kusch S, Acevedo-Garcia J, Wu H, Panstruga R. Biotrophy at its best: novel findings and unsolved mysteries of the Arabidopsis-powdery mildew pathosystem. Arabidopsis Book. 2016;14:e0184.

Lallement PA, Brouwer B, Keech O, Hecker A, Rouhier N. The still mysterious roles of cysteine-containing glutathione transferases in plants. Front Pharmacol. 2014;5:192.

Langlois-Meurinne M, Gachon CM, Saindrenan P. Pathogen-responsive expression of glycosyltransferase genes *UGT73B3* and *UGT73B5* is necessary for resistance to *Pseudomonas syringae* pv *tomato* in Arabidopsis. Plant Physiol. 2005;139:1890–901.

Laporte D, Olate E, Salinas P, Salazar M, Jordana X, Holuigue L. Glutaredoxin GRXS13 plays a key role in protection against photooxidative stress in Arabidopsis. J Exp Bot. 2012;63:503–15.

Lee S, Seo CH, Lim B, Yang JO, Oh J, Kim M, et al. Accurate quantification of transcriptome from RNA-Seq data by effective length normalization. Nucleic Acids Res. 2011;39:e9.

Li J, Brader G, Kariola T, Palva ET. WRKY70 modulates the selection of signaling pathways in plant defense. Plant J. 2006;46:477–91.

Li J, Brader G, Palva ET. The WRKY70 transcription factor: a node of convergence for jasmonate-mediated and salicylate-mediated signals in plant defense. Plant Cell. 2004;16:319–31.

Love MI, Huber W, Anders S. Moderated estimation of fold change and dispersion for RNA-seq data with DESeq2. Genome Biol. 2014;15:550.

Miya A, Albert P, Shinya T, Desaki Y, Ichimura K, Shirasu K, et al. CERK1, a LysM receptor kinase, is essential for chitin elicitor signaling in Arabidopsis. Proc Natl Acad Sci U S A. 2007;104:19613–8.

Mortazavi A, Williams BA, Mccue K, Schaeffer L, Wold B. Mapping and quantifying mammalian transcriptomes by RNA-Seq. Nat Methods. 2008;5:621–8.

Nawrath C, Metraux JP. Salicylic acid induction-deficient mutants of Arabidopsis express *PR-2* and *PR-5* and accumulate high levels of camalexin after pathogen inoculation. Plant Cell. 1999;11:1393–404.

Ndamukong I, Abdallat AA, Thurow C, Fode B, Zander M, Weigel R, et al. SA-inducible Arabidopsis glutaredoxin interacts with TGA factors and suppresses JA-responsive PDF1.2 transcription. Plant J. 2007;50:128–39.

Nishimura MT, Stein M, Hou BH, Vogel JP, Edwards H, Somerville SC. Loss of a callose synthase results in salicylic acid-dependent disease resistance. Science. 2003;301:969–72.

Ramonell K, Berrocal-Lobo M, Koh S, Wan J, Edwards H, Stacey G, et al. Loss-of-function mutations in chitin responsive genes show increased susceptibility to the powdery mildew pathogen *Erysiphe cichoracearum*. Plant Physiol. 2005;138:1027–36.

Rustérucci C, Aviv DH, Holt BF III, Dangl JL, Parker JE. The disease resistance signaling components components *EDS1* and *PAD4* are essential regulators of the cell death pathway controlled by *LSD1* in Arabidopsis. Plant Cell. 2001;13:2211–24.

Shim JS, Jung C, Lee S, Min K, Lee YW, Choi Y, et al. *AtMYB44* regulates *WRKY70* expression and modulates antagonistic interaction between salicylic acid and jasmonic acid signaling. Plant J. 2013;73:483–95.

Takahashi T, Shibuya H, Ishikawa A. SOBIR1 contributes to non-host resistance to *Magnaporthe oryzae* in Arabidopsis. Biosci Biotechnol Biochem. 2016;80: 1577–9.

Tang D, Ade J, Frye CA, Innes RW. Regulation of plant defense responses in Arabidopsis by EDR2, a PH and START domain-containing protein. Plant J. 2005;44:245–57.

Tang D, Ade J, Frye CA, Innes RW. A mutation in the GTP hydrolysis site of Arabidopsis dynamin-related protein 1E confers enhanced cell death in response to powdery mildew infection. Plant J. 2006;47:75–84.

Underwood W, Somerville SC. Perception of conserved pathogen elicitors at the plasma membrane leads to relocalization of the Arabidopsis PEN3 transporter. Proc Natl Acad Sci U S A. 2013;110:12492–7.

Vogel JP, Raab TK, Schiff C, Somerville SC. PMR6, a pectate lyase-like gene required for powdery mildew susceptibility in Arabidopsis. Plant Cell. 2002;14: 2095–106.

Wan J, Zhang XC, Neece D, Ramonell KM, Clough S, Kim SY, et al. A LysM receptor-like kinase plays a critical role in chitin signaling and fungal resistance in Arabidopsis. Plant Cell. 2008;20:471–81.

Wang G, Zhang G, Wu M. CLE peptide signaling and crosstalk with phytohormones and environmental stimuli. Front Plant Sci. 2015;6:1211.

Wang W, Wen Y, Berkey R, Xiao S. Specific targeting of the Arabidopsis resistance protein RPW8.2 to the interfacial membrane encasing the fungal Haustorium renders broad-spectrum resistance to powdery mildew. Plant Cell. 2009;21: 2898–913.

Wang X, Hou S, Wu Q, Lin M, Acharya BR, Wu D, et al. IDL6-HAE/HSL2 impacts pectin degradation and resistance to *Pseudomonas syringae* pv *tomato* DC3000 in Arabidopsis leaves. Plant J. 2017;89:250–63.

Wang Y, Cheng X, Shan Q, Zhang Y, Liu J, Gao C, et al. Simultaneous editing of three homoeoalleles in hexaploid bread wheat confers heritable resistance to powdery mildew. Nat Biotechnol. 2014;32:947–51.

Wen Y, Wang W, Feng J, Luo MC, Tsuda K, Katagiri F, et al. Identification and utilization of a sow thistle powdery mildew as a poorly adapted pathogen to dissect post-invasion non-host resistance mechanisms in Arabidopsis. J Exp Bot. 2011;62:2117–29.

Wrzaczek M, Brosche M, Salojarvi J, Kangasjarvi S, Idanheimo N, Mersmann S, et al. Transcriptional regulation of the CRK/DUF26 group of receptor-like protein kinases by ozone and plant hormones in Arabidopsis. BMC Plant Biol. 2010; 10:95.

Wu G, Liu S, Zhao Y, Wang W, Kong Z, Tang D. ENHANCED DISEASE RESISTANCE4 associates with CLATHRIN HEAVY CHAIN2 and modulates plant immunity by regulating relocation of EDR1 in Arabidopsis. Plant Cell. 2015;27:857–73.

Xiao S, Calis O, Patrick E, Zhang G, Charoenwattana P, Muskett P, et al. The atypical resistance gene, *RPW8*, recruits components of basal defence for powdery mildew resistance in Arabidopsis. Plant J. 2005;42:95–110.

Yeh YH, Chang YH, Huang PY, Huang JB, Zimmerli L. Enhanced Arabidopsis pattern-triggered immunity by overexpression of cysteine-rich receptor-like kinases. Front Plant Sci. 2015;6:322.

Yeh YH, Panzeri D, Kadota Y, Huang YC, Huang PY, Tao CN, et al. The Arabidopsis malectin-like/LRR-RLK IOS1 is critical for BAK1-dependent and BAK1-independent pattern-triggered immunity. Plant Cell. 2016;28:1701–21.

Young MD, Wakefield MJ, Smyth GK, Oshlack A. Gene ontology analysis for RNA-seq: accounting for selection bias. Genome Biol. 2010;11:R14.

Zeilmaker T, Ludwig NR, Elberse J, Seidl MF, Berke L, Van Doorn A, et al. DOWNY MILDEW RESISTANT 6 and DMR6-LIKE OXYGENASE 1 are partially redundant but distinct suppressors of immunity in Arabidopsis. Plant J. 2015;81:210–22.

Zhang L-L, Ma X-F, Zhou B-B, Zhao J-Q, Fan J, Huang F, et al. EDS1-mediated basal defense and SA-signaling contribute to post-invasion resistance against tobacco powdery mildew in *Arabidopsis*. Physiol Mol Plant Pathol. 2015;91:120–30.

Zhang X, Han X, Shi R, Yang G, Qi L, Wang R, et al. Arabidopsis cysteine-rich receptor-like kinase 45 positively regulates disease resistance to *Pseudomonas syringae*. Plant Physiol Biochem. 2013;73:383–91.

Zhou M, Lu Y, Bethke G, Harrison BT, Hatsugai N, Katagiri F, et al. WRKY70 prevents axenic activation of plant immunity by direct repression of *SARD1*. New Phytol. 2018;217:700–12.

Zhou N, Tootle TL, Tsui F, Klessig DF, Glazebrook J. PAD4 functions upstream from salicylic acid to control defense responses in Arabidopsis. Plant Cell. 1998;10:1021–30.